RESEARCH

CircWDR26 regulates endometrial carcinoma progression via miR-212-3p-mediated typing genes MSH2

Tao-Xiang Lei[1], De-Jian He[2], Jian Cao[3] and Wang-Gui Lv[1*]

Abstract

Background: Circular RNAs (circRNA) are important in mediating tumor progression, but their roles in endometrial carcinoma (EC) are not fully understood yet. Many circRNAs are dysregulated and may contribute to EC progression. The functions of circWDR26 in EC remain unknown.

Methods: The expression of circWDR26 in EC and adjacent normal tissues, and cell lines was determined by qPCR. The proliferation, apoptosis, migration, and invasion of EC cells was examined by CCK-8 assay, flow cytometry, wound healing assay and Transwell assay. The interaction between circWDR26, MSH2 and miR-212-3p was determined by luciferase assay. EC cells were inoculated into nude mice and tumor burden was determined by measuring tumor dimensions, size, and weight. The proliferative marker Ki67 in EC tissue was determined by immunohistochemistry.

Results: The expression of circWDR26 in EC tissues or cell lines was higher than in the normal tissue or endometrial epithelial cells. Downregulation of circWDR26 resulted in attenuated proliferation, increased apoptosis, reduced migration and invasion of EC cells. Mechanistically, circWDR26 targeted and suppressed the expression of miR-212-3p. We further found that MSH2 was the novel target of miR-212-3p and was upregulated by circWDR26 via inhibiting miR-212-3p. In vivo experiment demonstrated that circWDR26 was essential for EC tumor growth.

Conclusion: circWDR26 promoted EC progression by regulating miR-212-3p/MSH2 axis and provided novel insights into anti-cancer treatment.

Keywords: Endometrial carcinoma, CircWDR26, MiR-212-3p, MSH2

Introduction

Endometrial cancer (EC) is the most common gynecological cancer in high-income countries. More than 300,000 women were diagnosed with, and nearly 70,000 died of EC worldwide annually. Although the early stage ECs have relatively good prognosis, the high-grade ECs tend to recur [1]. Surgery is the initial treatment for EC, around 90% EC patients have some form of surgery [2].

Additionally, adjuvant chemotherapy increases survival in EC, especially those with late stage EC (Stage III/IV) [2–4]. However, the oncogenesis of EC is not fully understood yet, studies are still needed to elucidate the pathogenesis of EC and to identify new targets for EC treatment.

The functions of circular RNAs (circRNA) in cancers start to emerge in recent years. CircRNAs exert multiple roles in oncogenesis by promoting malignant cell growth and proliferation, increasing cellular invasiveness, sustaining cellular stemness, circumventing cellular senescence and death, and fostering drug resistance [5, 6]. CircRNAs also hold the potential to be novel biomarkers for cancer [7–9]. Research on circRNAs in EC is still

*Correspondence: lvwanggui370@163.com

[1] Department of Gynecological Oncology Surgery, Chenzhou First People's Hospital (The First Affiliated Hospital of Xiangnan University), No.849 Youth Avenue, Chenzhou 423000, Hunan Province, China
Full list of author information is available at the end of the article

Lei *et al. European Journal of Medical Research*   (2022) 27:135

Page 2 of 11

limited. Chen et al. analyzed the transcriptome of circR-NAs in EC and found significant difference from normal tissue [10]. The expression of circWDR26 is elevated in EC [11, 12], but its roles and underlying mechanisms is not well studied yet.

One of the action models of circRNAs is as a sponge for microRNAs (miRNA) [13, 14]. As a competing endogenous RNA (ceRNA), circRNA directly binds to miRNA(s) with complementary sequence, and thus suppresses its activities, including promoting mRNA degradation [15]. hsa_circRNA_0001776 suppresses growth and induces apoptosis of EC by targeting miR-182 [16]. Moreover, circRNA WHSC1 regulates miR-646 to facilitate EC progression [17]. MiRNAs play versatile roles in carcinogenesis [18]. MiR-449a and miR-145-5p can serve as prognostic biomarkers for EC [19]. MiR-1271 targets CDK1 to suppress EC cell growth and induce apoptosis [20]. MiR-212-3p suppresses tumor progression in multiple cancers by targeting different molecules. miR-212-3p attenuated hepatocellular carcinoma cell growth and invasion by inhibiting CTGF [21], while in ovarian cancer, miR-212-3p can target MAP3K3 [22]. However, the exact role of miR-212-3p in EC is not known. Exploiting bioinformatic tool, we found a potential binding site between circWDR26 and miR-212-3p, which is not reported yet, and the role of circWDR26/miR-212-3p interaction in EC oncogenesis remains unknown.

The most well-known function of miRNA is directly binding to mRNA and promotes its degradation, suppressing gene translation and function [23]. miR-212-3p directly suppresses the expression connective tissue growth factor interrupt the proliferation and invasion of hepatocellular carcinoma [21]. In addition, miR-212-3p attenuates group 3 medulloblastoma progression via targeting nuclear factor I/B [24]. Again, with the bioinformatic tool, we identified a potential binding site in *MSH2*, which are tightly associated with malignancy [25–28], for miR-212-3p. However, the role of MSH2 in EC is unexplored yet. Therefore, it would be interesting to elaborate the relationship between circWDR26, miR-212-3p, and MSH2 in EC development.

In our current study, we explored the role and underlying regulatory mechanism of circWDR26 in EC oncogenesis. We found that circWDR26 promoted the proliferation, survival, migration, and invasion of EC cells through miR-212-3p/MSH2 axis, providing novel insights in the treatment of EC.

Materials and methods

Tissue specimen collection
Tumors and adjacent normal tissues ($n = 30$) used in this study were obtained from The First Affiliated Hospital of Xiangnan University. The adjacent normal tissues were at least 5 cm away from tumor tissues. All patients did not receive any tumor-related treatment, including radiotherapy and chemotherapy before tissue collection. Tissues were snap-frozen and stored in -80 °C. Lymph node metastasis was evaluated by diagnostic radiology and pathology. Moreover, the clinical characteristics of EC patients are provided in Table 2. The study was approved by The First Affiliated Hospital of Xiangnan University and performed in accordance with the provisions of the Declaration of Helsinki and Good Clinical Practice guidelines. Written informed consent was obtained from all patients.

Cell culture and transfection
Human endometrial cancer cell line RL95-2 (Catalog #CRL-1671, American Type Culture Collection, ATCC), Ishikawa (CL-0283, Procell Life Science & Technology Co., Ltd), HEC-1-A (Catalog #HTB-112, ATCC), and HEC-1B (Catalog #HTB-113, ATCC) were cultured in complete DMEM (10% FBS, 100 units/ml penicillin, and 100 μg/ml streptomycin) at 37 °C in an atmosphere containing 5% CO_2.

Human endometrial epithelial cells (hEEC) were isolated from endometrial specimens as previously described [29]. The endometrial tissue was minced in Ca^{2+}/Mg^{2+}-free PBS (Catalog #SH30256.01, Hyclone) and digested by type I collagenase (Sigma) and hyaluronidase for 1 h. Digested tissue were filtered through a 40-μm cell strainer (Falcon). The flow-through was discarded and materials remained in the filter were washout and cultured in stromal cell medium containing 67.5% complete DMEM (Catalog #12430054, Gibco), 22.5% MCDB-105 (Catalog #M6395, Sigma) at 37 °C for 1 h. Collected medium and unattached cells were centrifuged, resuspended in KSFM (Catalog #17005042, Gibco), and cultured for further experiments.

sh-circWDR26, pc-circWDR26, miR-212-3p mimic/inhibitor or the corresponding control plasmid were obtained from GenePharma Co., Ltd (Shanghai, China), and co-transfected into cells by Lipofectamine 2000 (Catalog #11668-030, Invitrogen) following manufacture's instruction. Cells were transfected with 2.5 μg plasmid and incubated for 48 h before further experiments. Transfection to cells in different plates was performed similarly with adjustment of the amount of all materials proportionally.

Cell proliferation assay
Measurement of cell viability was performed by cell counting kit 8 (CCK-8) from Abcam (Catalog #ab228554) following manufacturer's instruction. Briefly, 10^4 cells were seeded in a 96-well plate with clear bottom. Ten microliter CCK-8 solution was added, and cells were

Lei *et al. European Journal of Medical Research*   (2022) 27:135

Page 3 of 11

incubated for 3 h at 37 °C free of light. The absorbance was measured at 460 nm.

Colony formation assay

Cells were mixed with 1% agarose solution (Low gelling temperature agarose, Catalog #A9045, Sigma) and 2000 cells/well were seeded in 6-well plate pre-coated with 1% agarose. Cells were cultured for 2 weeks to allow colonies to form. Plates were fixed, followed by staining with 0.2% crystal violet solution (Catalog #C0775, Sigma). Excess staining was removed with 3 PBS washes, and cells were imaged with ChemiDoc scanner (BioRad). Cell colonies were counted by ImageJ software.

Apoptosis assay

Apoptosis was determined by flow cytometry using Annexin V antibody and propidium iodide (PI). Single cell suspension was prepared by trypsinizing and ice-cold PBS washes. Cells were then incubated with Annexin V FITC (ANNEX300F, Bio-Rad) and ReadiDrop™ PI (1351101, Bio-Rad) for 1 h at 4 °C protect from light. Apoptotic cells were detected with Beckman Coulter Gallios Flow Cytometer and analyzed using FlowJo software (FlowJo, Ashland, USA).

Wound healing assay

Seed 2×10^5 cells into each well of 12-well culture plate, and culture for 18–24 h to reach 100% confluence. The cell layer was scraped with a 1-mm pipette tip, the detached cells washed out, and 1.5 mL fresh medium replenished. The cells were imaged using microscope as 0 h. Cells were incubated for another 48 h and imaged under microscope.

Transwell assay

Cells were suspended in FBS-free media and seeded in top chambers of the Transwell plates, and 0.5 mL complete medium were added into the lower well as attractant. The inserts were taken out carefully 24 h later. The cells were fixed in 4% paraformaldehyde and stained with 1% crystal violet. The inserts were washed in PBS and the cells in the inner compartment of the inserts were gently removed. Cell number on the outer surface of the insert was counted and imaged under microscope.

Western blotting

Protease inhibitor cocktail (cOmplete, Roche) containing RIPA buffer was used to extract cellular protein. A total of 20 µg proteins were loaded and separated by 10% SDS-PAGE and transferred onto polyvinylidene difluoride membrane. Blots was developed using enhanced chemiluminescence kits (Cat. #1705060S, BIO-RAD) as substrates and were visualized and captured by a ChemicDoc

XRS system (Bio-Rad) and quantified by ImageJ software. Following antibodies were diluted at a ratio of 1:1000 for western blot experiment: MSH2 (Cat. #2017, Cell Signaling Technology), β-actin (Cat. #3700, Cell Signaling Technology).

RNA isolation and real-time quantitative PCR (qPCR)

RNA was extracted from snap-frozen tissues and cells by RNeasy Mini Kit (Cat. No. 74104, QIAGEN) following manufacturer's instruction. The quality and concentration of total RNA were checked by agarose gel electrophoresis and absorbance using NanoDrop 2000 spectrophotometer, respectively. cDNA was synthesized using High-Capacity cDNA Reverse Transcription Kit (Cat. #4368814, Applied Biosystems) from 1 µg of total RNA following manufacture's instruction. The real-time qPCR was performed using SsoAdvanced Universal SYBR Green Supermix (Cat. #1725270, BIO-RAD) as following: 94 °C for 10 min, followed by 40 cycles of 94 °C for 15 s, 60 °C for 1 min. Glyceraldehyde 3-phosphate dehydrogenase (GAPDH) served as reference gene. The relative gene expression was calculated by $2^{-\Delta\Delta Ct}$. Primer information is provided in Table 1.

Dual luciferase reporter gene assay

The binding sites between circWDR26, *TP53, LDLR, PUM2, LATS2, FOXN3* or *MSH2* and miR-212-3p were predicted by Starbase (https://starbase.sysu.edu.cn/). Predicted binding motifs and corresponding mutant (MUT) in above candidate genes were inserted into psiCHECK2 luciferase reporter vector (Promega, China). HEK293T cells were co-transfected miR-212-3p mimic with above luciferase reporter plasmids for 48 h. The relative ratio of Rluc/Luc was analyzed using the Dual-Luciferase reporter system (Promega, USA) as per the instructions.

Table 1 Primers used in qRT-PCR

Gene	Primers (5′–3′)
circWDR26	F 5′- TGATGGCACTAAACTAGCAACAG -3′
	R 5′-TCCAATAGTTTAGATCGGGAAGC -3′
miR-212-3p	F 5′- CGCGAGATCAGAAGGTGATT -3′
	RT 5′- GTCGTATCCAGTGCAGGGTCCGAG GTATTCGCACTGGATACGACAGCCAC-3′
U6	F 5′- CTCGCTTCGGCAGCACA-3′
	R 5′- AACGCTTCACGAATTTGCGT-3′
MSH2	F 5′- TGGATCAGGTGGAAAACCAT-3′
	R 5′- ATCCAAACTGTGCACTGGAA-3′
GAPDH	F 5′- CCAGGTGGTCTCCTCTGA -3′
	R 5′- GCTGTAGCCAAATCGTTGT-3′

Lei *et al. European Journal of Medical Research*   (2022) 27:135

Page 4 of 11

Xenograft EC mouse model

All animal experiments were performed in accordance with protocols approved by The First Affiliated Hospital of Xiangnan University. Balb/c female nude mice (6–8 weeks old) were obtained from Beijing Experimental Animal Center. Mice were maintained in a 12-h light/ dark, 20–25 °C and 50–65 humidity specific pathogen-free animal facility with adequate food and water ad libitum and were acclimated for 1 week before tumor cell inoculation. A total of 1×10^6 HEC-1-A cells expressing either sh-NC or sh-circWDR26 were injected subcutaneously. The dimensions of tumors were measured once a week. On day 35, mice were euthanized before they become moribund. Tumors were isolated for further analysis.

Statistical analysis

Experiment was repeated for at least three times. Data were shown as mean ± SD. One-way ANOVA or Student's t-test was used for statistical analysis with GraphPad Prism 8 software. $p < 0.05$ is considered statistically significant.

Results

The expression of circWDR26 is elevated in EC

To investigate the expression pattern of circWDR26 in EC tissue, we compared the levels of circWDR26 in 30 normal tissues and 30 EC tissues. The expression of circWDR26 was dramatically upregulated in EC tissue (Fig. 1A). We next inquired whether the expression of circWDR26 changes along with tumor progression. The result indicated that the level of circWDR26 in EC tissue in late stages (Stage III–IV) were higher than in early stages (Stages I–II) (Fig. 1B). Level of circWDR26 was also positively correlated with metastasis of EC to lymph node. Tumor tissues from patients with lymphatic metastasis showed higher expression of circWDR26 than those without lymphatic metastasis (Fig. 1C). CircWDR26
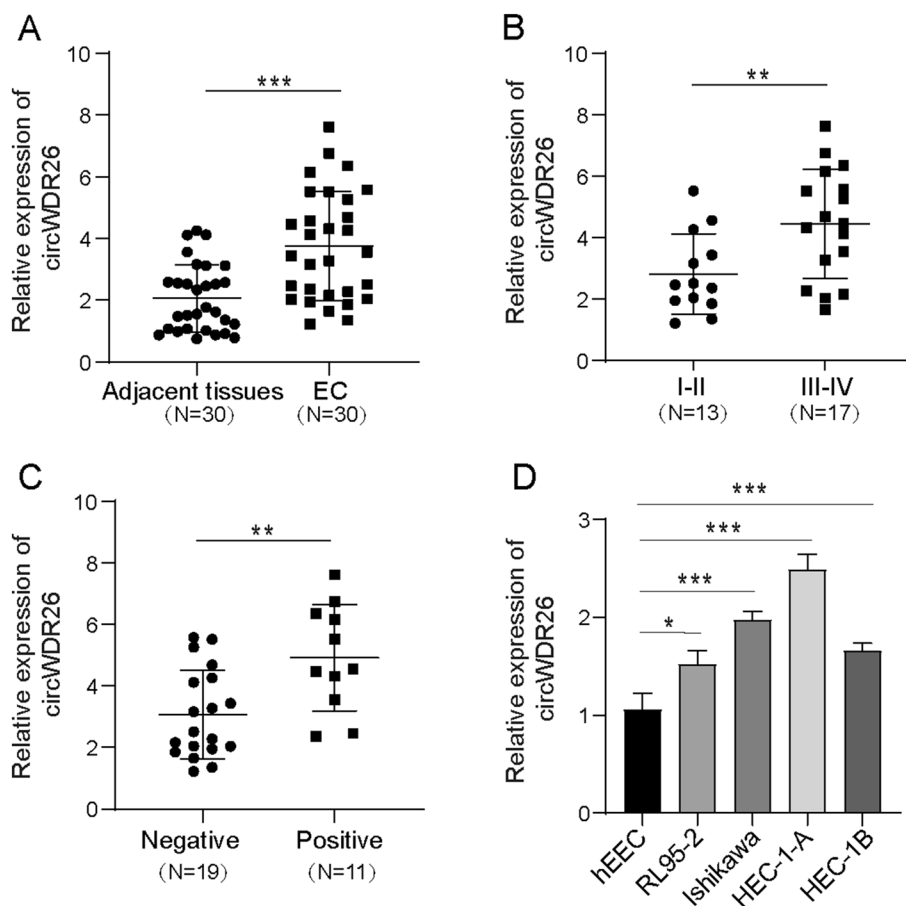

Fig. 1 The expression of circWDR26 is elevated in EC. **A** The level of circWDR26 in normal tissue (NT) and EC tissue (EC) was determined by qPCR. **B** The level of circWDR26 in early stage (I–II) and late stage (III–IV) EC tissues was determined by qPCR. **C** The expression level of circWDR26 in tissues from patients with or without lymph node metastasis was determined by qPCR. **D** The expression of circWDR26 in hEEC and EC cell lines was determined by qPCR. *$p < 0.05$, **$p < 0.01$, ***$p < 0.001$

Lei *et al. European Journal of Medical Research*   (2022) 27:135

Page 5 of 11

expression in hEEC and EC cells were also examined, the level of circWDR26 was upregulated in all four EC cell lines compared with hEEC (Fig. 1D). Moreover, the clinicopathological characteristics, including age, tumor size, FIGO stage, differentiation, and lymphatic metastasis, of the 30 EC patients are provided in Table 2. These data demonstrated that the expression circWDR26 was upregulated in EC and was associated with tumor progression and metastasis, implying its role in EC pathogenesis.

To examine its functions in EC, circWDR26 expression in EC cells were silenced by shRNA. As excepted, sh-circWDR26 effectively suppressed the expression of circWDR26 (Fig. 2A). The proliferation rate of EC cells was significantly attenuated by sh-circWDR26, compared with sh-NC (Fig. 2B). The clonogenic ability of EC cells was dramatically suppressed following circWDR26 downregulation (Fig. 2C). In addition, EC cells with lower circWDR26 expression exhibited higher rate of apoptosis (Fig. 2D). The migration capacity, as indicated in wound healing assay, of EC cells was decreased in sh-circWDR26 cells (Fig. 2E). Moreover, the invasion capacity of EC cells was also inhibited in cells expressing sh-circWDR26 (Fig. 2F). These data indicated that circWDR26 plays critical roles in proliferation, survival, migration, and invasion of EC cells.

CircWDR26 acts as sponge of miR-212-3p
Next, we explored the possible targets of circWDR26 in EC cells. Bioinformatic analysis revealed that miR-212-3p contains potential binding site with circWDR26 (Fig. 3A). Luciferase activity in cells expressing WT circWDR26 was significantly suppressed by miR-212-3p mimic, while that in cells expressing MUT circWDR26 remained unchanged (Fig. 3B). In sh-circWDR26 expressing cells, the level of miR-212-3p was significantly increased, while overexpressing of circWDR26 reduced the expression of miR-212-3p (Fig. 3C). Consistently, significant reduction of miR-212-3p in EC tissue, compared with normal tissue, was observed (Fig. 3D). The expression level of circWDR26 was negatively associated with that of miR-212-3p (Fig. 3E). These findings suggested that miR-212-3p is a target of circWDR26 in EC.

MiR-212-3p directly targets MSH2 in EC
Several potential targets (TP53, PUM2, MSH2, LDLR, LATS2, and FOXN3) of miR-212-3p were predicted by the Starbase software (Fig. 4A). Subsequently, we further examined if these candidate genes were regulated by miR-212-3p using dual-luciferase assays. Results revealed that miR-212-3p mimic reduced the luciferase activity of WT TP53 and MSH2, but there was no statistical differences in other candidate genes and MUT (Fig. 4B). Similarly, miR-212-3p inhibitor promoted the expression

Table 2 The clinical characteristics of EC patients

Characteristics	EC	
	Case ($N = 30$)	%
Age (year)		
≤ 50	14	46.67
> 50	16	53.33
Tumor size (cm)		
≤ 4	18	60.00
> 4	12	40.00
FIGO stage		
I–II	13	43.33
III–IV	17	56.67
Differentiation		
High and medium differentiation	16	53.33
Low and undifferentiation	14	46.67
Lymph nude metastasis		
Positive	11	36.67
Negative	19	63.33

EC endometrial carcinoma, *FIGO* Federation of Gynecology and Obstetrics

of MSH2, but miR-212-3p mimic decreased the levels of MSH2 (Fig. 4C). The protein levels of MSH2 were consistently upregulated by miR-212-3p inhibitor and downregulated by miR-212-3p mimic (Fig. 4D). Concomitant with reduced expression of miR-212-3p in EC, the expression of MSH2 was dramatically increased in EC tissue, compared with normal tissue (Fig. 4E), and MSH2 expression was negatively correlated with the expression of miR-212-3p (Fig. 4F). These results demonstrated that miR-212-3p negatively regulated MSH2 expression in EC.

CircWDR26 promotes EC progression by regulating miR-212-3p/MSH2 axis
To investigate whether miR-212-3p/MSH2 axis is required for circWDR26-mediated EC progression, we first examined the expression of MSH2 following manipulation of circWDR26 and miR-212-3p. Knockdown of circWDR26 decreased the expression of MSH2, while additional miR-212-3p inhibitor reversed the suppression of MSH2 in sh-circWDR26 cells (Fig. 5A). Cell proliferation was attenuated in EC cells expressing sh-circWDR26, while miR-212-3p inhibitor offset the inhibitory effect of sh-circWDR26 (Fig. 5B). The suppressed clonogenic capacity of EC cells in sh-circWDR26 was also enhanced with the addition of miR-212-3p inhibitor (Fig. 5C). Moreover, loss of circWDR26 promoted apoptosis, but further inhibition of miR-212-3p in these cells prevented them from apoptosis (Fig. 5D). sh-circWDR26 reduced migration of EC cells, while miR-212-3p inhibitor enhanced their
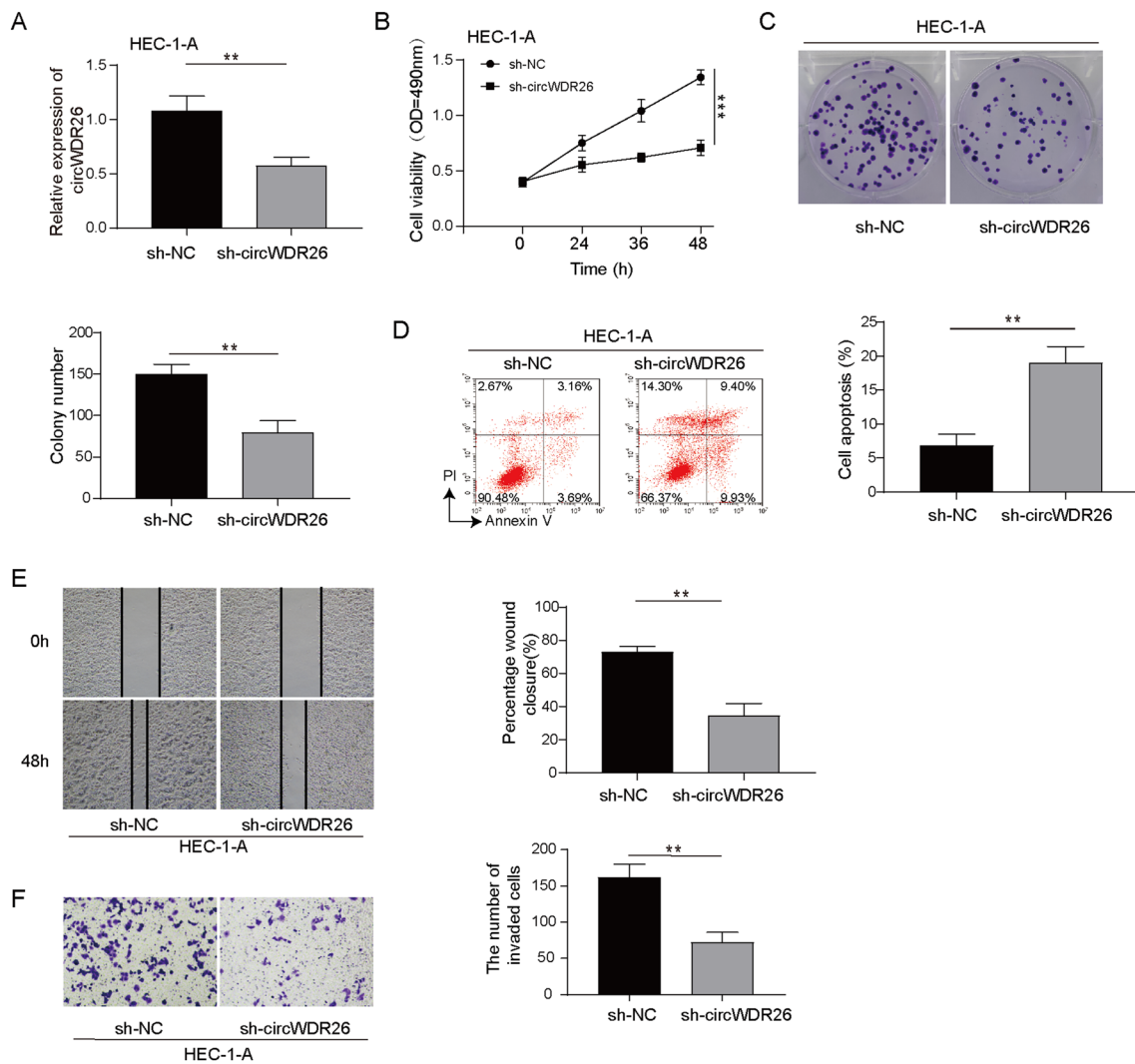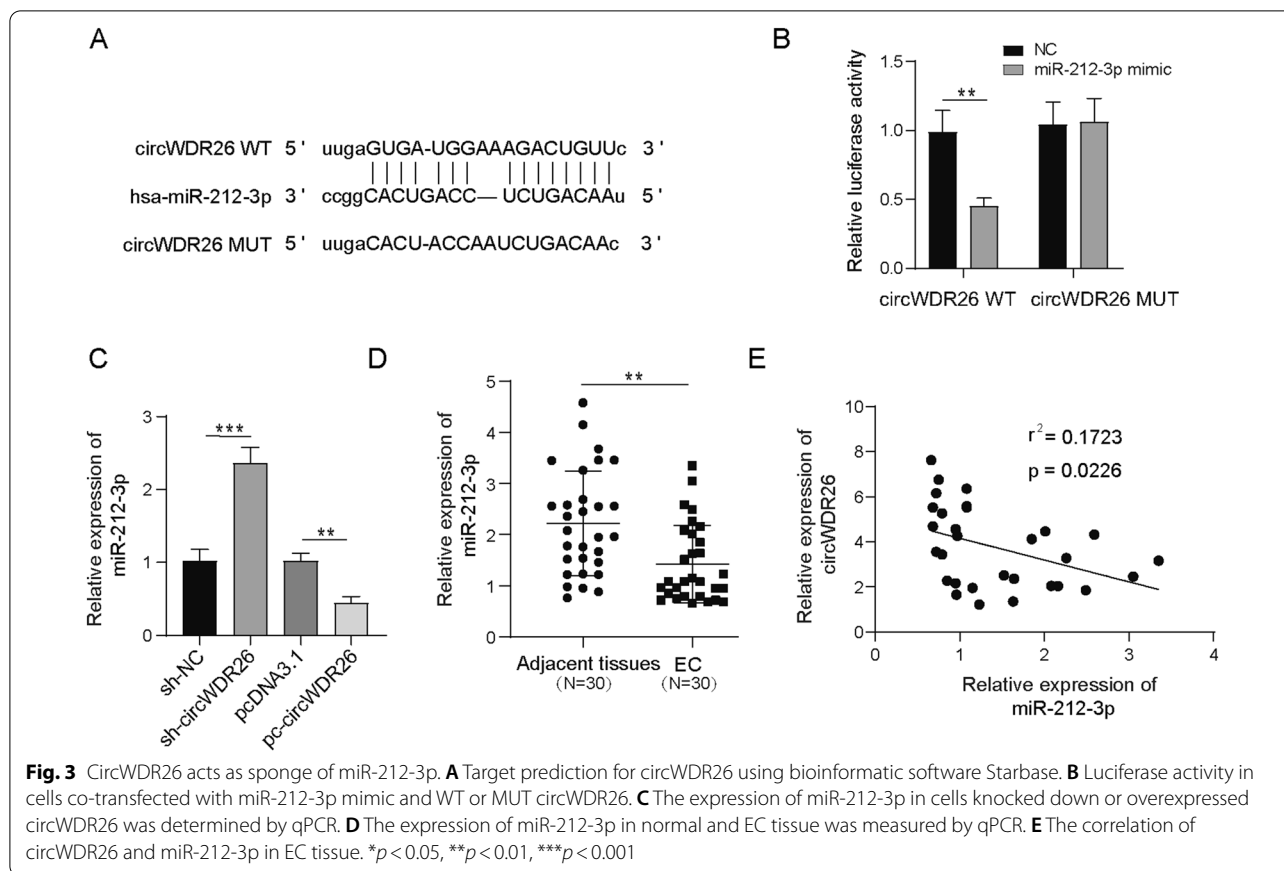
Fig. 2 Loss of circWDR26 suppresses the proliferation, migration and invasion, and promotes apoptosis of EC cells. **A** Knockdown efficiency of circWDR26 was determined by qPCR. **B** CCK-8 assay for cell viability of sh-NC or sh-circWDR26 EC cells. **C** Colony formation of sh-NC or sh-circWDR26 EC cells. **D** Apoptosis was determined by flow cytometry stained with PI and Annexin V antibody. **E** Migration capacity of EC cells was determined by wound healing assay. **F** EC cell invasion was measured by transwell assay. ******$p < 0.01$, *******$p < 0.001$

migratory activity (Fig. 5E). Similarly, invasiveness of EC cells was suppressed by sh-circWDR26, but miR-212-3p inhibitor attenuated the suppressive activity caused by loss of circWDR26 (Fig. 5F). Collectively, these data indicated that circWDR26 regulated the expression of MSH2 through miR-212-3p, and miR-212-3p was indispensable for its regulation of EC cell proliferation, apoptosis, migration, and invasion.

Loss of circWDR26 attenuated EC tumor growth in vivo

Our previous data showed important role of circWDR26 for EC cells, we next investigated if circWDR26 is essential for EC tumor growth in vivo. EC cells expressing control shRNA or circWDR26-targeting shRNA were inoculated into nude mice. The tumor volume was measured once a week. Sh-circWDR26 tumors had significant slower growth rate than the control tumors (Fig. 6A), which was consistent with the tumor size and weight (Fig. 6B and C) at the end point. Immunohistochemistry

Fig. 3 CircWDR26 acts as sponge of miR-212-3p. **A** Target prediction for circWDR26 using bioinformatic software Starbase. **B** Luciferase activity in cells co-transfected with miR-212-3p mimic and WT or MUT circWDR26. **C** The expression of miR-212-3p in cells knocked down or overexpressed circWDR26 was determined by qPCR. **D** The expression of miR-212-3p in normal and EC tissue was measured by qPCR. **E** The correlation of circWDR26 and miR-212-3p in EC tissue. *$p < 0.05$, **$p < 0.01$, ***$p < 0.001$
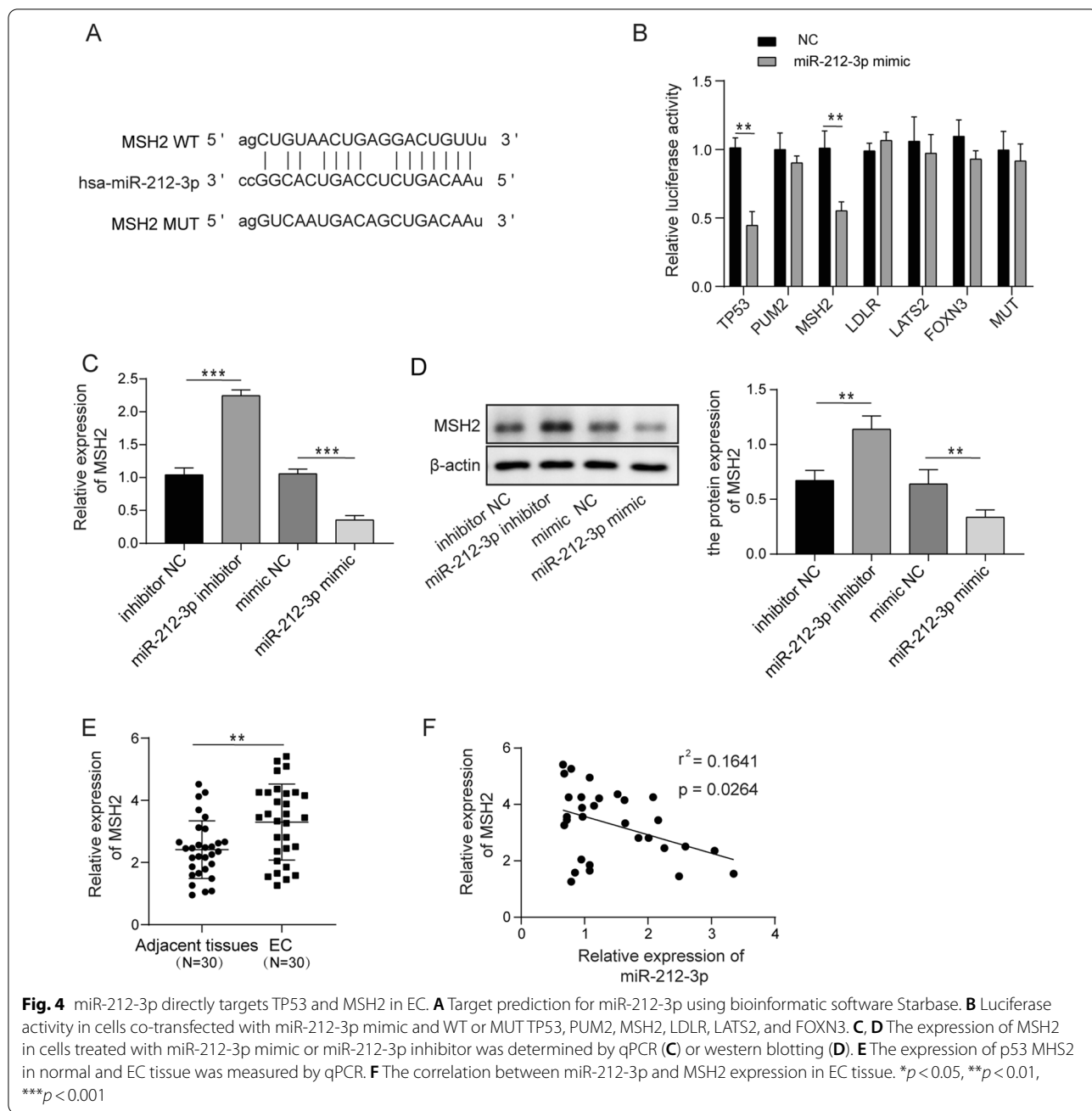
assay showed decreased level of proliferation marker Ki67 in sh-circWDR26 tumor (Fig. 6D). The expression of circWDR26 and its downstream effectors miR-212-3p, MSH2 in tumor tissues was examined by qPCR. Concomitant with reduced circWDR26 in sh-circWDR26 tumor, miR-212-3p expression was upregulated, while MSH2 was downregulated (Fig. 6E). Accordingly, the protein level of MSH2 were reduced significantly in sh-circWDR26 tumor tissues, when compared with sh-NC tumor tissues (Fig. 6F). Therefore, our data demonstrated that circWDR26 regulates EC tumor progression in vivo through a miR-212-3p/MSH2 axis.

Discussion

EC remains a huge health concern as around 300,000 new cases were diagnosed annually and nearly 70,000 died from EC worldwide [1]. Metastasis and recurrence are common in patients with high-grade EC [2]. Plenty studies in recent years have revealed the versatile functions of circRNAs in the pathogenesis of EC [30, 31]. Among them, the role of circWDR26 in the pathogenesis of EC is still poorly understood. Our current study discovered novel roles of circWDR26 in promoting the development of EC through a miR-212-3p/MSH2 axis-dependent manner.
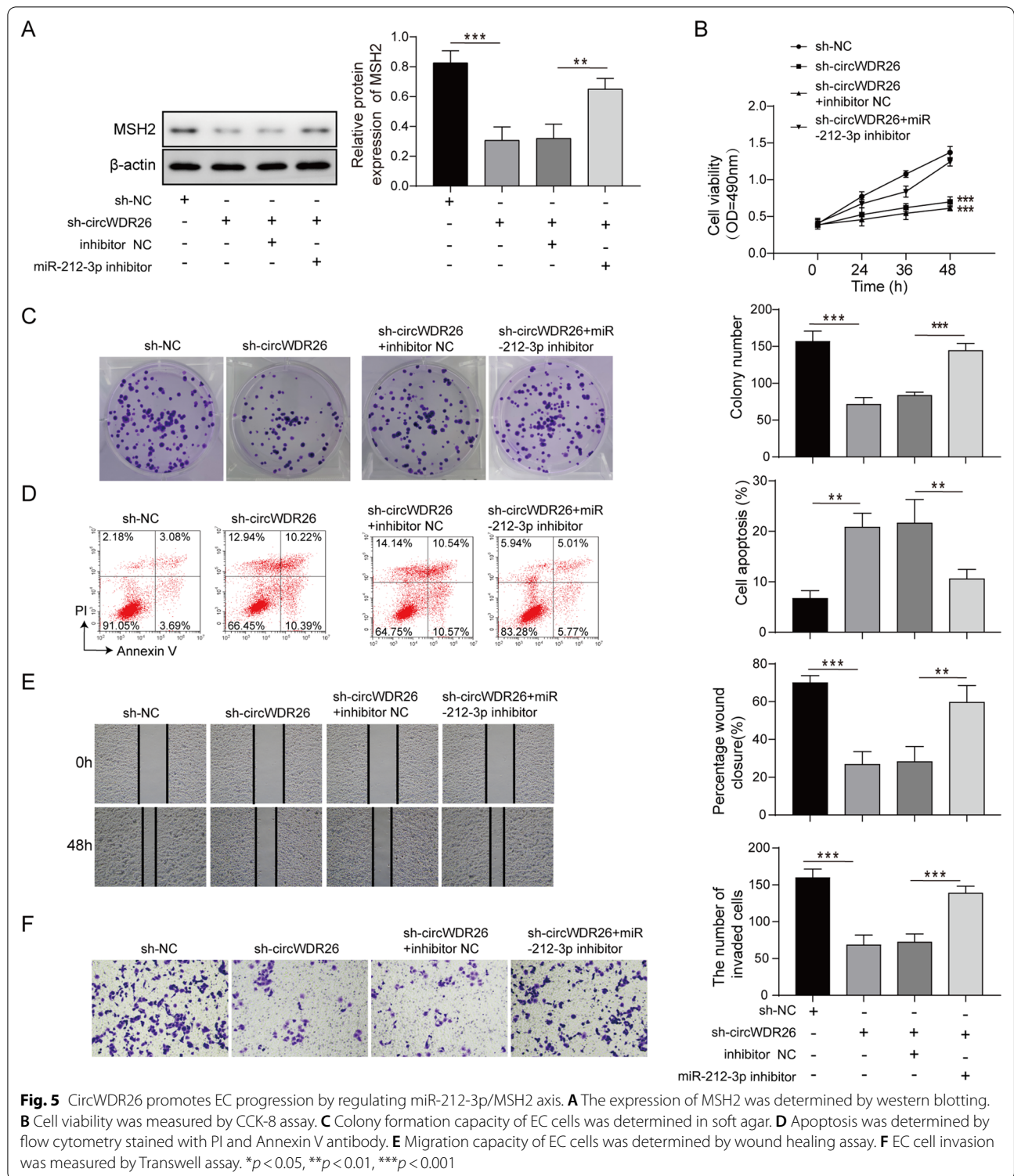
The important roles of circRNAs in cancers are emerging [5, 32, 33], but more researches are still required to understand their roles and underlying mechanisms which regulate tumor progression. WDR26 was upregulated in multiple cancers to promote tumor progression [30, 31]. Upregulated WDR26 may also lead to elevation of circWDR26. Previous studies have reported the roles of circWDR26 in promoting EC progression by activating Wnt/β-catenin pathway and IGF1R/PI3K/Akt pathways [11, 12]. Here we found circWDR26 promoted cultured EC cell proliferation, survival, migration and invasion. Given its important roles in EC, it is not surprising that the expression of circWDR26 was elevated in tumor. CircWDR26 expression in EC cells was upregulated and was elevated in EC tissues, and it was upregulated along with tumor progression, as circWDR26 in tissues from late stages were higher than that from early stages. The expression of circWDR26 showed association with lymph node metastasis of EC. Reduced expression of circWDR26 in EC cells dramatically suppressed tumor growth. Collectively our data demonstrated that

Fig. 4 miR-212-3p directly targets TP53 and MSH2 in EC. **A** Target prediction for miR-212-3p using bioinformatic software Starbase. **B** Luciferase activity in cells co-transfected with miR-212-3p mimic and WT or MUT TP53, PUM2, MSH2, LDLR, LATS2, and FOXN3. **C, D** The expression of MSH2 in cells treated with miR-212-3p mimic or miR-212-3p inhibitor was determined by qPCR (**C**) or western blotting (**D**). **E** The expression of p53 MHS2 in normal and EC tissue was measured by qPCR. **F** The correlation between miR-212-3p and MSH2 expression in EC tissue. *$p < 0.05$, **$p < 0.01$, ***$p < 0.001$

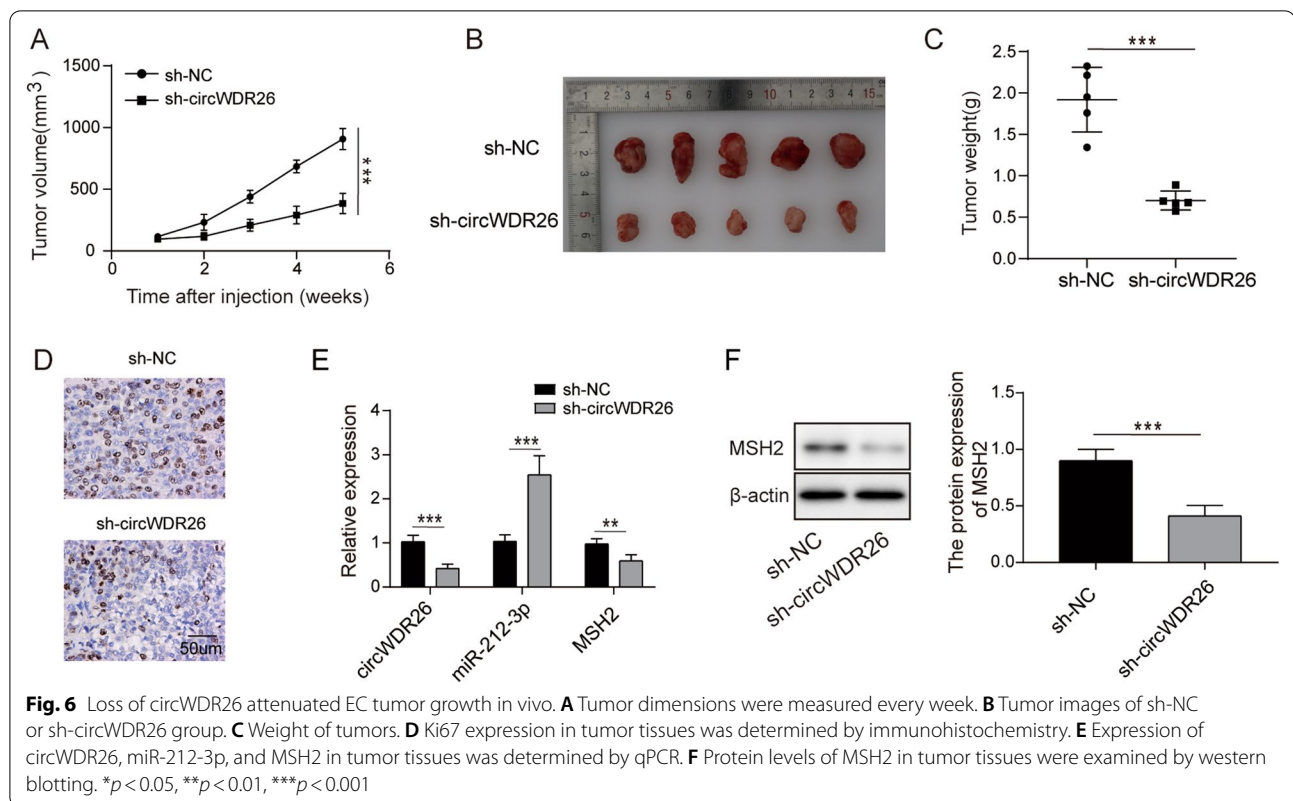circWDR26 has multiple functions in EC and is essential for EC progression.

Many studies have revealed the classical model of circRNA function as miRNA sponges [13, 14]. Here we found circWDR26 regulated the activity of its target miR-212-3p in a similar way. Using bioinformatic tools, we found circWDR26 contains potential binding site for miR-212-3p, which was further experimentally validated by dual-luciferase assay. The level of miR-212-3p was also downregulated after circWDR26 knockdown. Moreover,

loss of circWDR26 attenuated EC progression and can be rescued by miR-212-3p inhibitor, further emphasizing the regulatory role of circWDR26 on miR-212-3p expression to promote EC progression. miR-212-3p exhibits inhibitory activity in proliferation and migration of human hepatocellular carcinoma [21]. The expression of miR-212-3p is downregulated in ovarian cancer cells and tumor tissues [34], and miR-212-3p suppressed the progression of high-grade serous ovarian cancer [22]. Although miR-212-3p showed broad tumor suppressor

Lei *et al. European Journal of Medical Research*   (2022) 27:135

Page 9 of 11

Fig. 5 CircWDR26 promotes EC progression by regulating miR-212-3p/MSH2 axis. **A** The expression of MSH2 was determined by western blotting. **B** Cell viability was measured by CCK-8 assay. **C** Colony formation capacity of EC cells was determined in soft agar. **D** Apoptosis was determined by flow cytometry stained with PI and Annexin V antibody. **E** Migration capacity of EC cells was determined by wound healing assay. **F** EC cell invasion was measured by Transwell assay. *$p < 0.05$, **$p < 0.01$, ***$p < 0.001$

activities in various cancers, its role in EC has not been reported yet. MiRNA usually directly binds to its mRNA targets and leads to its degradation, downregulating the expression of target genes [35]. We identified multiple candidate genes (TP53, PUM2, MSH2, LDLR, LATS2, and FOXN3) that contain potential binding site for miR-212-3p. While TP53 and MSH2, among them, were suppressed by miR-212-3p mimic in dual-luciferase assay.

Fig. 6 Loss of circWDR26 attenuated EC tumor growth in vivo. **A** Tumor dimensions were measured every week. **B** Tumor images of sh-NC or sh-circWDR26 group. **C** Weight of tumors. **D** Ki67 expression in tumor tissues was determined by immunohistochemistry. **E** Expression of circWDR26, miR-212-3p, and MSH2 in tumor tissues was determined by qPCR. **F** Protein levels of MSH2 in tumor tissues were examined by western blotting. *$p < 0.05$, **$p < 0.01$, ***$p < 0.001$

Moreover, we found TP53 was upregulated in EC, which is consistent with previous report [36], demonstrating that overexpression of TP53 is related to malignancy. On the contrary, we found that TP53 could play the role of antitumor in subsequent functional experiments, which is consistent with a previous report [37]. Meanwhile, it is well known that TP53 exerts the tumor suppressor role in cancers. These data suggested that the role of TP53 is controversial in EC and requires further comprehensive investigation in the future. Therefore, we focused on the function of MSH2 in EC in our current study. The expression of MSH2 was directly downregulated or upregulated by miR-212-3p mimic and miR-212-3p inhibitor, respectively. Inhibition of miR-212-3p led to concomitant MSH2 upregulation and EC progression. Germline MSH2 mutation was associated with higher risks of ovarian and endometrial cancer [25, 27], and the expression of MSH2 is associated with poor prognosis of uterine corpus endometrial carcinoma with a hazard ratio of 1.56 [38]. These data demonstrated that miR-212-3p regulated EC progression by MSH2. Taken together, our current study reveals that circWDR26 directly regulates the miR-212-3p-p53/MSH2 axis to affect EC tumor progression. This will help us understand the mechanism of EC

tumors and provide new insights for the future treatment of EC.

Author contributions
W-GL: guarantor of integrity of the entire study. T-XL: study concepts; study design. D-JH: definition of intellectual content; literature research. JC: clinical studies; experimental studies. T-XL, D-JH: data acquisition; data analysis. W-GL, JC: statistical analysis; manuscript preparation; manuscript editing. D-JH, JC: manuscript review. All authors read and approved the final manuscript.

Availability of data and materials
All data generated or analyzed during this study are included in this published article.

Declarations

Ethics approval and consent to participate
Ethical approval of this study was granted by The First Affiliated Hospital of Xiangnan University and performed in accordance with the provisions of the

Lei *et al. European Journal of Medical Research*   (2022) 27:135

Page 11 of 11

Declaration of Helsinki and Good Clinical Practice guidelines. Written informed consent was obtained from all patient.

Consent for publication
The informed consent obtained from study participants.

Competing interests
The authors declare no competing interests.

Author details
[1]Department of Gynecological Oncology Surgery, Chenzhou First People's Hospital (The First Affiliated Hospital of Xiangnan University), No.849 Youth Avenue, Chenzhou 423000, Hunan Province, China. [2]Department of Emergency, Chenzhou First People's Hospital (The First Affiliated Hospital of Xiangnan University), Chenzhou 423000, Hunan Province, China. [3]Medical Imaging Center, Chenzhou Fourth People's Hospital, Chenzhou 423000, Hunan Province, China.

References
1. Amant F, Mirza MR, Koskas M, Creutzberg CL. Cancer of the corpus uteri. Int J Gynaecol Obstet. 2018;143(Suppl 2):37–50.
2. Vale CL, Tierney J, Bull SJ, Symonds PR. Chemotherapy for advanced, recurrent or metastatic endometrial carcinoma. Cochrane Database Syst Rev. 2012. https://doi.org/10.1002/14651858.CD003915.pub4.
3. Galaal K, Al Moundhri M, Bryant A, Lopes AD, Lawrie TA. Adjuvant chemotherapy for advanced endometrial cancer. Cochrane Database Syst Rev. 2014. https://doi.org/10.1002/14651858.CD010681.pub2.
4. Colombo N, Preti E, Landoni F, Carinelli S, Colombo A, Marini C, et al. Endometrial cancer: ESMO clinical practice guidelines for diagnosis, treatment and follow-up. Ann Oncol. 2013;24(Suppl 6):vi33–8.
5. Su M, Xiao Y, Ma J, Tang Y, Tian B, Zhang Y, et al. Circular RNAs in cancer: emerging functions in hallmarks, stemness, resistance and roles as potential biomarkers. Mol Cancer. 2019;18(1):90.
6. Liu J, Zhang X, Yan M, Li H. Emerging role of circular RNAs in cancer. Front Oncol. 2020;10:663.
7. Brown JR, Chinnaiyan AM. The potential of circular RNAs as cancer biomarkers. Cancer Epidemiol Biomarkers Prev. 2020;29(12):2541–55.
8. Lei B, Tian Z, Fan W, Ni B. Circular RNA: a novel biomarker and therapeutic target for human cancers. Int J Med Sci. 2019;16(2):292–301.
9. Wang S, Zhang K, Tan S, Xin J, Yuan Q, Xu H, et al. Circular RNAs in body fluids as cancer biomarkers: the new frontier of liquid biopsies. Mol Cancer. 2021;20(1):13.
10. Chen BJ, Byrne FL, Takenaka K, Modesitt SC, Olzomer EM, Mills JD, et al. Analysis of the circular RNA transcriptome in endometrial cancer. Oncotarget. 2018;9(5):5786–96.
11. Shen Q, He T, Yuan H. Hsa_circ_0002577 promotes endometrial carcinoma progression via regulating miR-197/CTNND1 axis and activating Wnt/beta-catenin pathway. Cell Cycle. 2019;18(11):1229–40.
12. Wang Y, Yin L, Sun X. CircRNA hsa_circ_0002577 accelerates endometrial cancer progression through activating IGF1R/PI3K/Akt pathway. J Exp Clin Cancer Res. 2020;39(1):169.
13. Memczak S, Jens M, Elefsinioti A, Torti F, Krueger J, Rybak A, et al. Circular RNAs are a large class of animal RNAs with regulatory potency. Nature. 2013;495(7441):333–8.
14. Hansen TB, Jensen TI, Clausen BH, Bramsen JB, Finsen B, Damgaard CK, et al. Natural RNA circles function as efficient microRNA sponges. Nature. 2013;495(7441):384–8.
15. Verduci L, Strano S, Yarden Y, Blandino G. The circRNA-microRNA code: emerging implications for cancer diagnosis and treatment. Mol Oncol. 2019;13(4):669–80.
16. Jia Y, Liu M, Wang S. CircRNA hsa_circRNA_0001776 inhibits proliferation and promotes apoptosis in endometrial cancer via downregulating LRIG2 by sponging miR-182. Cancer Cell Int. 2020;20:412.
17. Liu Y, Chen S, Zong ZH, Guan X, Zhao Y. CircRNA WHSC1 targets the miR-646/NPM1 pathway to promote the development of endometrial cancer. J Cell Mol Med. 2020;24(12):6898–907.
18. Yanokura M, Banno K, Kobayashi Y, Kisu I, Ueki A, Ono A, et al. MicroRNA and endometrial cancer: roles of small RNAs in human tumors and clinical applications (review). Oncol Lett. 2010;1(6):935–40.
19. Wu X, Han Y, Liu F, Ruan L. Downregulations of miR-449a and miR-145-5p act as prognostic biomarkers for endometrial cancer. J Comput Biol. 2020;27(5):834–44.
20. Li L, Qu YW, Li YP. Over-expression of miR-1271 inhibits endometrial cancer cells proliferation and induces cell apoptosis by targeting CDK1. Eur Rev Med Pharmacol Sci. 2017;21:2816–22.
21. Chen JQ, Ou YL, Huang ZP, Hong YG, Tao YP, Wang ZG, et al. MicroRNA-212-3p inhibits the proliferation and invasion of human hepatocellular carcinoma cells by suppressing CTGF expression. Sci Rep. 2019;9(1):9820.
22. Zhang L, Zhang Y, Wang S, Tao L, Pang L, Fu R, et al. MiR-212-3p suppresses high-grade serous ovarian cancer progression by directly targeting MAP3K3. Am J Transl Res. 2020;12(3):875–88.
23. O'Brien J, Hayder H, Zayed Y, Peng C. Overview of microRNA biogenesis, mechanisms of actions, and circulation. Front Endocrinol. 2018;9:402.
24. Perumal N, Kanchan RK, Doss D, Bastola N, Atri P, Venkata RC, et al. MiR-212-3p functions as a tumor suppressor gene in group 3 medulloblastoma via targeting nuclear factor I/B (NFIB). Acta Neuropathol Commun. 2021. https://doi.org/10.1186/s40478-021-01299-z.
25. Ramsoekh D, Wagner A, van Leerdam ME, Dooijes D, Tops CM, Steyerberg EW, et al. Cancer risk in MLH1, MSH2 and MSH6 mutation carriers; different risk profiles may influence clinical management. Hered Cancer Clin Pract. 2009;7(1):17.
26. Parc Y, Boisson C, Thomas G, Olschwang S. Cancer risk in 348 French MSH2 or MLH1 gene carriers. J Med Genet. 2003;40:208–13.
27. Bonadona V, Bonaïti B, Olschwang S, Grandjouan S, Huiart L, Longy M, et al. Cancer risks associated with germline mutations in MLH1, MSH2, and MSH6 genes in lynch syndrome. JAMA. 2011;305(22):2304–10.
28. Olivier M, Hollstein M, Hainaut P. TP53 mutations in human cancers: origins, consequences, and clinical use. Cold Spring Harb Perspect Biol. 2010;2(1): a001008.
29. Schatz F, Soderland C, Hendricks-Munoz KD, Gerrets RP, Lockwood CJ. Human endometrial endothelial cells: isolation, characterization, and inflammatory-mediated expression of tissue factor and type 1 plasminogen activator inhibitor. Biol Reprod. 2000;62:691–7.
30. Tu J, Yang H, Chen Y, Chen Y, Chen H, Li Z, et al. Current and future roles of circular RNAs in normal and pathological endometrium. Front Endocrinol. 2021;12: 668073.
31. Guo J, Tong J, Zheng J. Circular RNAs: a promising biomarker for endometrial cancer. Cancer Manag Res. 2021;13:1651–65.
32. Kristensen LS, Hansen TB, Veno MT, Kjems J. Circular RNAs in cancer: opportunities and challenges in the field. Oncogene. 2018;37(5):555–65.
33. Song H, Liu Q, Liao Q. Circular RNA and tumor microenvironment. Cancer Cell Int. 2020;20:211.
34. Lu X, Wang F, Fu M, Li Y, Wang L. [ARTICLE WITHDRAWN] long noncoding RNA KCNQ1OT1 accelerates the progression of ovarian cancer via microRNA-212-3/LCN2 axis. Oncol Res. 2020;28(2):135–46.
35. Gebert LFR, MacRae IJ. Regulation of microRNA function in animals. Nat Rev Mol Cell Biol. 2019;20(1):21–37.
36. Mirakhor Samani S, Ezazi Bojnordi T, Zarghampour M, Merat S, Fouladi DF. Expression of p53, Bcl-2 and Bax in endometrial carcinoma, endometrial hyperplasia and normal endometrium: a histopathological study. J Obstet Gynaecol. 2018;38(7):999–1004.
37. Wild PJ, Ikenberg K, Fuchs TJ, Rechsteiner M, Georgiev S, Fankhauser N, et al. p53 suppresses type II endometrial carcinomas in mice and governs endometrial tumour aggressiveness in humans. EMBO Mol Med. 2012;4(8):808–24.
38. Qiu W, Ding K, Liao L, Ling Y, Luo X, Wang J. Analysis of the expression and prognostic value of msh2 in pan-cancer based on bioinformatics. Biomed Res Int. 2021;2021:9485273.

Publisher's Note
Springer Nature remains neutral with regard to jurisdictional claims in published maps and institutional affiliations.